Vol 15 No 9, September 2006
1009-1963/2006/15(09)/2146-05

Chinese Physics

© 2006 Chin. Phys. Soc.
and IOP Publishing Ltd

Crystal field analysis of the magnetization curves of R_2Fe_{17} and $R_2Fe_{17}H_3$ (R=Tb,Ho,Er)*

Ma Ru-Gui(马如贵)[a], Yan Yu(闫　羽)[a,b]†,
Zhang Yan-Xiang(张艳香)[c], Du Xiao-Bo(杜晓波)[a],
Wang Xiang-Qun(王向群)[a], Su Feng(苏　峰)[a], and Jin Han-Min(金汉民)[a]

[a] *Department of Physics, Jilin University, Changchun* 130021, *China*
[b] *State Key Laboratory for Superhard Materials, Jilin University, Changchun* 130012,*China*
[c] *Jilin Provincial Institute of Education, Changchun* 130022, *China*

(Received 8 February 2006; revised manuscript received 24 March 2006)

In this paper the values of the crystalline-electric-field parameters $A_{\rm nm}$ for R_2Fe_{17} and $R_2Fe_{17}H_3$ (R=Tb,Ho,Er) are evaluated by fitting calculations to the magnetization curves measured on the single crystal at several temperatures. The fitted $A_{\rm nm}$ for R_2Fe_{17} are strikingly different from those for the corresponding $R_2Fe_{17}H_3$. The energy gaps between the lowest four energy levels for Ho ions in Ho_2Fe_{17} can be reproduced by using the fitted $A_{\rm nm}$ and exchange field $2\mu_{\rm B}H_{\rm ex}$, which estimated from the fit of the temperature dependence of the spontaneous magnetization combined with inelastic neutron scattering experiment.

Keywords: magnetization curves, magnetic anisotropy, rare-earth compounds, crystalline-electric-field
PACC: 7560E, 7530G, 7550B, 7510D

1. Introduction

In the last decades, the magnetic properties of R_2Fe_{17} and their hydrides $R_2Fe_{17}H_3$ have been studied extensively.[1−11] Many experimental investigations of the intrinsic magnetic properties of $R_2Fe_{17}H_x$ (x = 0, 3, 5) single crystals have been reported.[1−8] The insertion of interstitial hydrogen elements in R_2Fe_{17} results in an apparent change of Curie temperature, saturation magnetization and magnetocrystalline anisotropy (MCA). There is no noticeable effect of hydrogenation on MCA in Rn_2Fe_{17} (Rn: nonmagnetic rare earths Y and Lu).[3,4] So it is interesting to analyse how the insertion of hydrogen can have an influence on MCA of the rare-earth ion in R_2Fe_{17}. It is known that the MCA of the rare-earth ion in the R–Fe(Co) intermetallic compounds originates from the crystalline-electric-field (CEF) interaction and the values of CEF parameters can be determined by fitting different experiments, such as the magnetization curves for single crystal and inelastic neutron scattering.[12,13]

This paper is to evaluate the values of CEF parameters A_{nm} of R_2Fe_{17} and $R_2Fe_{17}H_3$ (R = Er,Tb,Ho) from the experimental magnetization curves at several temperatures on the basis of the single-ion model and to analyse the experimental data.

2. Method of analysis

R_2Fe_{17} and their hydrides $R_2Fe_{17}H_3$ compounds have a Th_2Ni_{17}-type hexagonal structure with space group $P6_3/mmc$ for R = Tb, Ho and Er.[14,15] The R ion occupies two crystallographic different sites, 2b and 2d, both with the same point symmetry D_{3h}. In the coordinate system with the z and x axes along the c and a axes, the Hamiltonian of the CEF interaction for the R ions at the 2b and 2d sites are represented as

$$H_{\rm CEF} = \sum_{n=2,4,6} A_{n0}C_{n0} + A_{66}(C_{66} + C_{6-6}), \qquad (1)$$

where

$$C_{nm} = \sum_j [4\pi/(2n+1)]^{1/2} Y_{nm}(\theta_j, \varphi_j), \qquad (2)$$

$Y_{nm}(\theta_j, \varphi_j)$ are the spherical harmonics, and θ_j and φ_j are the polar and azimuthal angles of the position

*Project supported by Department of Science and Technology of Jilin Province and the National Natural Science Foundation of China (Grant No 10304006).
†Corresponding author. E-mail: yanyu@jlu.edu.cn

vector of jth 4f election. In fact, inelastic neutron scattering experiments on Ho_2Fe_{17} and Ho_2Co_{17} cannot distinguish a difference in the exchange interaction and in CEF interaction for R ion at the $2b$ and $2d$ sites,[15] and the calculation of a magnetization curve using the averaged CEF parameters for Ho_2Co_{17} compound gives rise to the same result as that obtained by using different values for the sites.[13] Averaged over the $2b$ and $2d$ sites, exchange field and CEF parameters were used in the calculations.

Neglecting the $R-R$ exchange interaction, we find that the Hamiltonian of the rare earth ion consists of the CEF interaction, the $R-$Fe exchange interaction and Zeeman energy, that is,

$$H = H_{\rm CEF} + 2\mu_{\rm B}\boldsymbol{S} \bullet \boldsymbol{H}_{\rm ex} + \mu_{\rm B}(\boldsymbol{L} + 2\boldsymbol{S}) \bullet \boldsymbol{H}. \quad (3)$$

The exchange field $\boldsymbol{H}_{\rm ex}$ is assumed to be proportional and anti-parallel to the magnetic moment of the Fe sublattice $\boldsymbol{M}_{\rm Fe}$. The matrix elements of Eq.(3) are calculated by using the irreducible-tensor-operator technique. For a given applied field $\boldsymbol{H}$ and a direction of $\boldsymbol{H}_{\rm ex}$, the eigenvalues E_i and eigenfunctions $|n_i> (i = 1, 2, \cdots, 2J+1)$ are obtained by diagonalizing the $(2J+1) \times (2J+1)$ matrix. The free energy for R_2Fe_{17} and their hydrides $R_2Fe_{17}H_3$ are given by

$$\begin{aligned} F(\boldsymbol{H}, \boldsymbol{M}_{\rm Fe}, T) = & -2k_{\rm B}T \ln Z + K_1(T) \sin^2 \theta_{\rm Fe} \\ & -\boldsymbol{M}_{\rm Fe}(T) \bullet \boldsymbol{H}, \end{aligned} \quad (4)$$

where

$$Z = \sum_i \exp(-E_i/k_{\rm B}T), \quad (5)$$

$K_1(T)$ is the MCA constant of the Fe sublattice. $M_{\rm Fe}(T/T_{\rm C})/M_{\rm Fe}(0)$ and $K_1(T/T_{\rm C})/K_1(0)$ for R_2Fe_{17} and $R_2Fe_{17}H_3$ are taken to be the same as those for Y_2Fe_{17}[5] and $Y_2Fe_{17}H_3$[3] respectively.[8,16] The values of $M_{\rm Fe}(0)$, which are adjusted around the value of Y_2Fe_{17}[3] and $Y_2Fe_{17}H_3$[3] for better fit, are listed in Table 1. The values of $M_{\rm Fe}(0)$ need to be adjusted again for a better fit of the experimental data for $Tb_2Fe_{17}H_x$ (x = 0,3) at 40 K. The readjusted value for Tb_2Fe_{17} and $Tb_2Fe_{17}H_3$ is 37.2 and 36.0$\mu_{\rm B}$/f.u. respectively. The value of $K_1(0)$ for R_2Fe_{17} and $R_2Fe_{17}H_3$ is taken to be –30 and –34 K/f.u. respectively, which are evaluated from the fit of the magnetization curve of Y_2Fe_{17} and $Y_2Fe_{17}H_3$ along the c axis at 4.2 K[3]. The equilibrium direction of $\boldsymbol{M}_{\rm Fe}$ is determined from minimization of the free energy. The magnetic moments of the rare-earth iron and of $R_2Fe_{17}H_x (x = 0,3)$ are given by

$$\boldsymbol{M}_{\rm R} = \mu_{\rm B} \sum_i \langle n_i \left| \boldsymbol{L} + 2\boldsymbol{S} \right| n_i \rangle \exp(E_i/k_{\rm B}T)/Z, \quad (6)$$

$$\boldsymbol{M} = 2\boldsymbol{M}_{\rm R} + \boldsymbol{M}_{\rm Fe}. \quad (7)$$

The values of the R–Fe exchange interaction $2\mu_{\rm B}H_{\rm ex}$ in R_2Fe_{17} and $R_2Fe_{17}H_3$ (R = Tb, Ho, Er) were estimated as follows. The values of $2\mu_{\rm B}H_{\rm ex}$ for Gd_2Fe_{17}, Ho_2Fe_{17} and Er_2Fe_{17} are evaluated to be 345, 260 and 250 K from the fit of the temperature dependence of the spontaneous magnetization.[5] The value of the exchange interaction acting on the spin of Gd ion in Gd_2Fe_{17}, which includes both the Gd–Fe and Gd–Gd contribution, is 384 K measured directly by means of the inelastic neutron scattering technique.[1] Compared with the fitted value of 345 K, the remaining 39 K would be the Gd–Gd contribution, which is roughly one order of magnitude smaller than Gd–Fe contribution as for the $GdFe_2$ and $Gd_2Fe_{14}B$ compounds.[17,18] It is known that the value of $2\mu_{\rm B}H_{\rm ex}$ decreases monotonically across the rare-earth serials from Pr to Er in many Rare-earth-Fe intermetallic compounds.[19,20] By extrapolating from the values of $2\mu_{\rm B}H_{\rm ex}$ for Gd_2Fe_{17}, Ho_2Fe_{17} and Er_2Fe_{17} to Tb_2Fe_{17}, the value for Tb_2Fe_{17} is estimated to be about 300 K. Inelastic neutron scattering experiment on Gd_2Fe_{17} and $Gd_2Fe_{17}D_3$ shows that the insertion of deuterium (D) leads to the reduction in $2\mu_{\rm B}H_{\rm ex}$ of about 6%. It is assumed that the reduction of $2\mu_{\rm B}H_{\rm ex}$ for a series of R_2Fe_{17} leaded by the insertion of deuterium and hydrogen is the same and the reduction is also 6% as for the Gd_2Fe_{17}. In this way the values of $2\mu_{\rm B}H_{\rm ex}$ for $Tb_2Fe_{17}H_3$, $Ho_2Fe_{17}H_3$ and $Er_2Fe_{17}H_3$ are estimated to be about 282, 245 and 235 K. The value of CEF parameters A_{nm} were evaluated by fitting calculations to the magnetization curves of R_2Fe_{17} and $R_2Fe_{17}H_3$ (R = Tb, Ho, Er) single crystal at different temperatures.

3. Results and discussion

Table 1 lists the fitted values of CEF parameters A_{nm} and $M_{\rm Fe}(0)$ for R_2Fe_{17} and $R_2Fe_{17}H_3$ (R = Tb, Ho, Er). It can be seen that the value of CEF parameters A_{nm} for $R_2Fe_{17}H_3$ are quite different from those for R_2Fe_{17}. This means that the insertion of hydrogen element in R_2Fe_{17} significantly affects A_{nm}. In this connection a Mössbauer study of ^{155}Gd in $Gd_2Fe_{17}H_x$ (x = 0,3,5) has shown that hydrogenation leads to a decrease of the electric field gradients at Gd ion site, which are proportional to A_{20}.[11]

Table 1. The fitted values of $M_{\rm Fe}(0)$ and CEF parameters A_{nm}

	$M_{\rm Fe}(0)$ /($\mu_{\rm B}$/f.u.)	A_{20} /K	A_{40} /K	A_{60} /K/	A_{64} /K
Tb_2Fe_{17}	36.5	−30	10	−600	−200
$Tb_2Fe_{17}H_3$	34.9	120	80	−30	500
Ho_2Fe_{17}	37.5	−240	−20	90	−160
$Ho_2Fe_{17}H_3$	37.2	−20	−10	−50	20
Er_2Fe_{17}	37.6	−10	−95	−10	−135
$Er_2Fe_{17}H_3$	35.5	10	30	10	−30

The uncertainty of each CEF parameter can be seen from the following data on Ho_2Fe_{17} at 4.2 K, which demonstrates the variation in the calculation of sensitively affected quantity when the value of each parameter is changed separately. An increase in $|A_{20}|$ by 12% or in $|A_{60}|$ by 33% or in $|A_{66}|$ by 13% changes the $M(\mu_0 H = 3\text{T})$ along the [001] axis from 4.6 to 4.3 or 5.0 or 4.3$\mu_{\rm B}$/f.u. respectively. A variation in A_{40} from –20 to –5 K changes the $M(\mu_0 H = 3\text{T})$ along the [001] axis from 4.6 to 4.4$\mu_{\rm B}$/f.u..

Figures 1–6 show the comparison of the calculations with experimental data. The solid circles represent the experimental data, and the curves the calculations. The calculations reproduce the experimental data well. Figures 1 and 2 show the magnetization curves along the crystal axes at 4.2 and 40 K for Tb_2Fe_{17} and $Tb_2Fe_{17}H_3$ respectively. The solid curves represent the calculations with $M_{\rm Fe}(0)$ listed in Table 1 and the dashed curves with the readjusted $M_{\rm Fe}(0)$ for a better fit of the experimental data at 40 K.

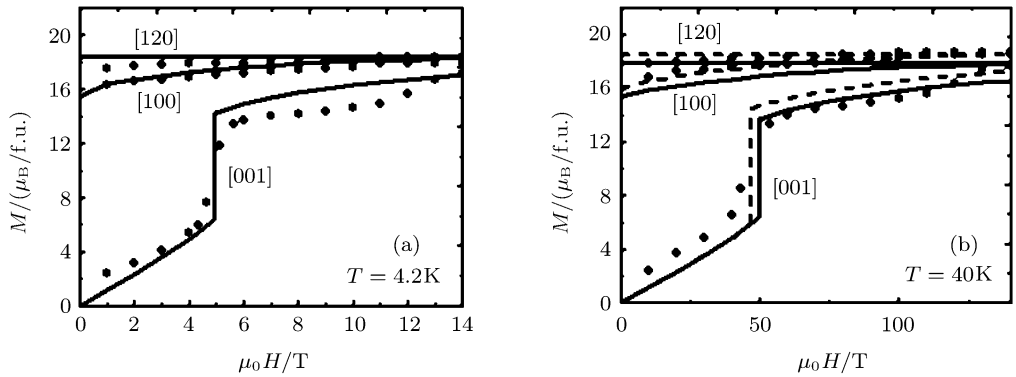


Fig.1. Magnetization curves of Tb_2Fe_{17} along the [100], [001] and [120] axes at 4.2 K (a) and 40 K (b). •••, experimental data from Ref.[3];——, the calculation ($M_{\rm Fe}(0) = 36.5\mu_{\rm B}$/f.u.); - - - , the calculation ($M_{\rm Fe}(0) = 37.2\mu_{\rm B}$/f.u.).

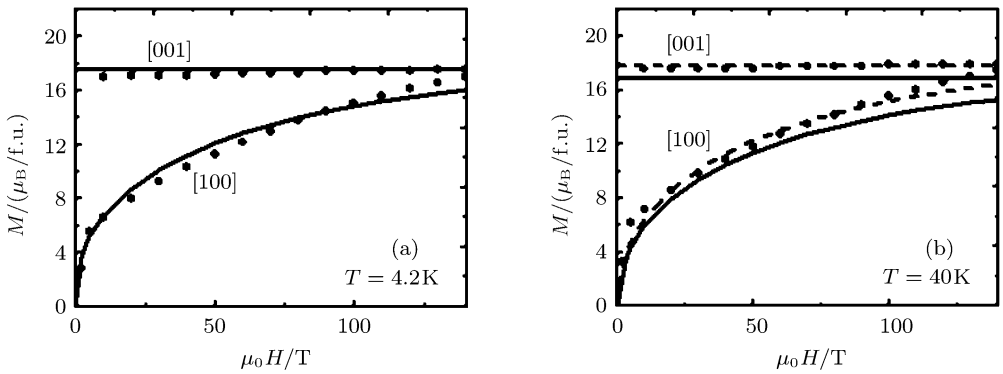


Fig.2. Magnetization curves of $Tb_2Fe_{17}H_3$ along [100] and [001] axes at 4.2 K (a) and 40 K (b). •••, experimental data from Ref.[3]; ——, the calculation ($M_{\rm Fe}(0) = 34.9\mu_{\rm B}$/f.u.); - - -, the calculation ($M_{\rm Fe}(0) = 36\mu_{\rm B}$/f.u.).

Figure 3 shows the magnetization curves along the crystal axes at 4.2, 40, 100 and 200 K for Ho_2Fe_{17}.

Figure 4 shows the magnetization curves along the crystal axes at 4.2 and 200 K for $Ho_2Fe_{17}H_3$.

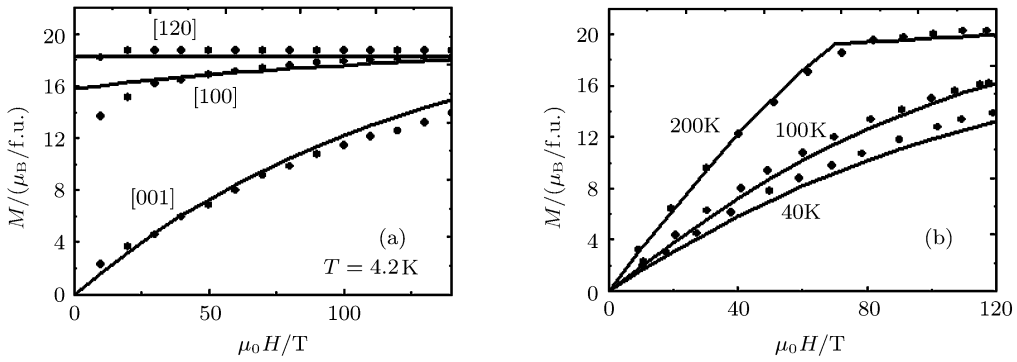


Fig.3. Magnetization curves of Ho_2Fe_{17} along the [100], [001] and [120] axes at 4.2 K (a) and along [001] axis at 40, 100 and 200 K (b). ●●●, experimental data from (a) Ref.[3] and (b) Ref.[8]; ——, the calculation.

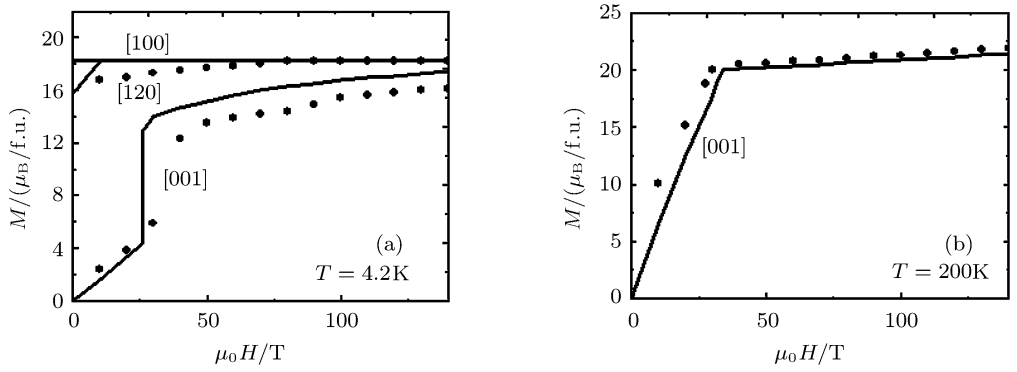


Fig.4. Magnetization curves of $Ho_2Fe_{17}H_3$ along the [100], [001] and [120] axes at 4.2 K (a) and along [001] axis at 200 K (b). ●●●, experimental data from (a) Ref.[3] and (b) Ref.[6]; ——, the calculation.

Figures 5 and 6 show the magnetization curves along the crystal axes at 4.2, 40, 80 and 200 K for Er_2Fe_{17} and $Er_2Fe_{17}H_3$ respectively. Our calculation shows that the sixth-order CEF parameter A_{60} plays a dominant role in reproducing the observed type-II first-order magnetization process along the [001] axis for Tb_2Fe_{17} and the [001] axis for $Ho_2Fe_{17}H_3$.

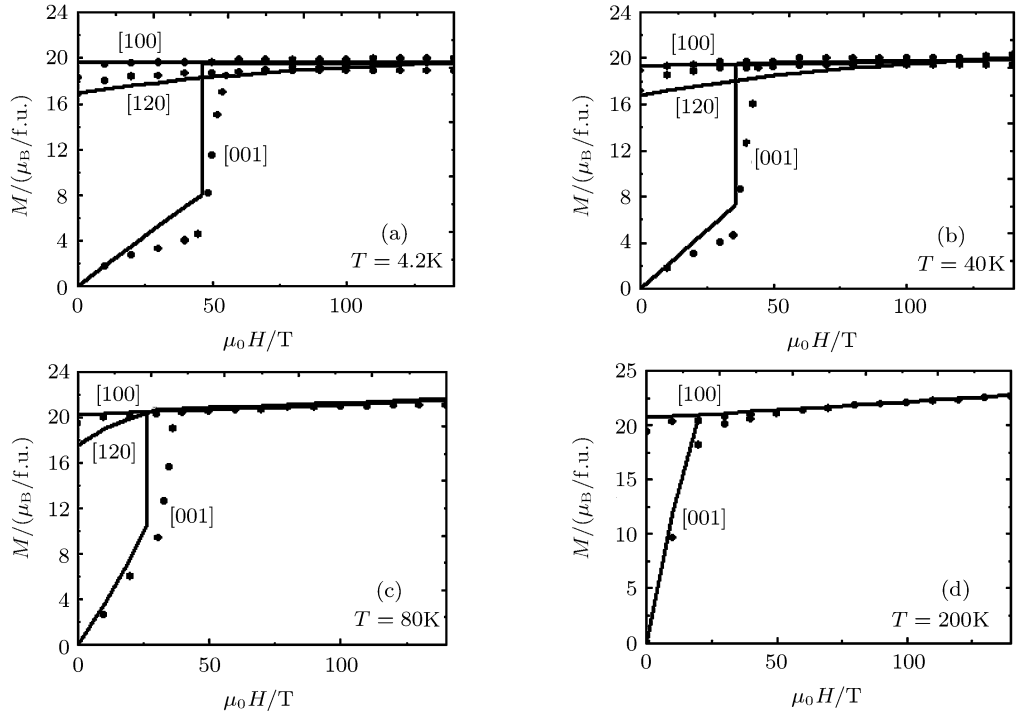


Fig.5. Magnetization curves of Er_2Fe_{17} along the [100], [001] and [120] axes at 4.2 (a), 40 (b) and 80 K (c) and along [100] and [001] axes at 200 K (d). ●●●, experimental data from Ref.[3]; ——, the calculation.

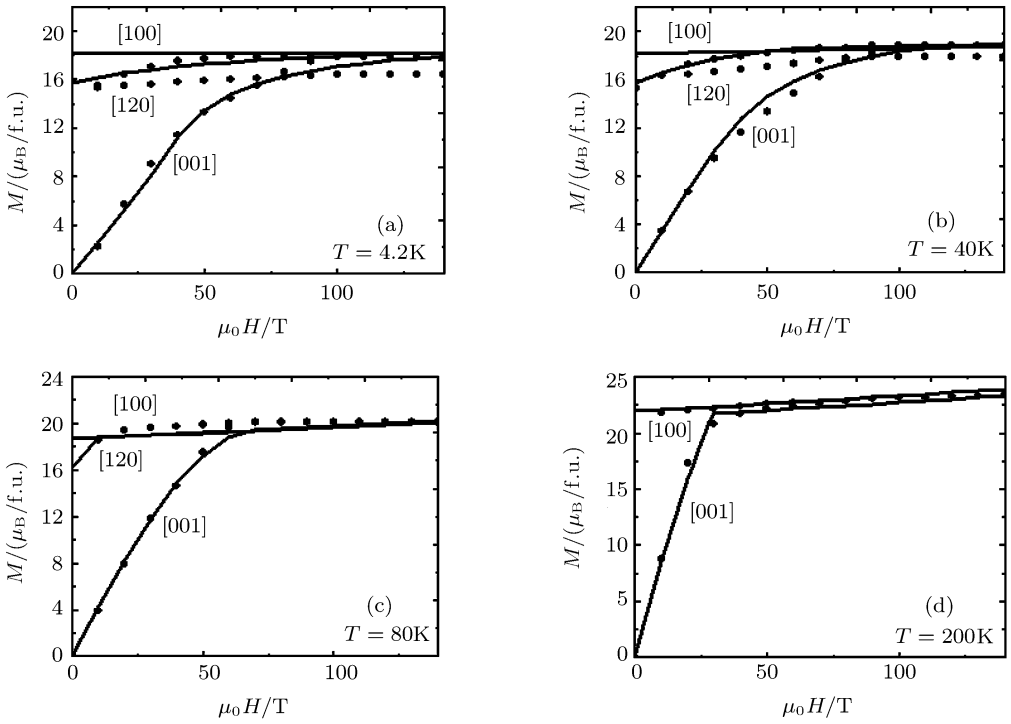


Fig.6. Magnetization curves of $Er_2Fe_{17}H_3$ along the [100], [001] and [120] axes at 4.2 (a), 40 (b) and 80 K (c) and along [100] and [001] axes at 200 K (d). ●●●, experimental data from Ref.[3]; ——, the calculation.

The calculated energy gaps between the lowest four energy levels for Ho_2Fe_{17} are $E_2 - E_1$=112.1K, $E_3 - E_2$=56.3K and $E_4 - E_3$=42.7K, which are in agreement with the experimental values of 96.3 K, 67.3 K and 55.7 K respectively.[15]

References

[1] Isnard O, Sippel A, Loewenhaupt M and Bewley R 2001 *J. Phys.: Condens. Matter* **13** 3533

[2] Tereshina I S, Nikitin S A, Verbetsky V N and Salamova A A 2002 *J. Alloys Compounds* **336** 36

[3] Tereshina I S, Nikitin S A, Skokov K P, Palewski T, Zubenko V V, Telegina I V, Verbetsky V N and Salamova A A 2003 *J. Alloys and Compounds* **350** 264

[4] Tereshina I S, Nikin S A, Stepien-Damm J, Gulay L D, Pankratov N Yu, Salamova A A, Verbetsky V N and Suski W 2001 *J. Alloys and Compounds* **329** 31

[5] Kamarad J, Mikulina O, Arnold Z, Garcia-Landa B and Ibarra M R 1999 *J. Appl. Phys.* **85** 4874

[6] Tereshina I S, Nikin S A, Stepien-Damm J, Suski W, Salamova A A and Verbetsky V N 2003 *J. Magn. Magn. Mater.* **258/259** 427

[7] Takeda K, Maeda T and Katayama T 1998 *J. Alloys Compounds* **281** 50

[8] Garcia-Landa B, Algarabel P A and Ibarra M R 1997 *Phys. Rev.* B **55** 8313.

[9] Nikitin S A, Ovtchenkov E A, Tereshina I S, Salamova A A and Verbetsky V N 1999 *J. Magn. Magn. Mater.* **195** 464

[10] Zhao T S, Lee T W, Pang K S and Lee J I 1995 *J. Magn. Magn. Mater.* **140/144** 1009

[11] Ianard O, Vulliet P, Blaise A, Sanchez J P, Miraglia S and Fruchart D 1994 *J. Magn. Magn. Mater.* **131** 83

[12] Su G, Yan Y, Xu S W, Du X B, Jin H M and Wang X Q 2005 *Chin. Phys.* **14** 2127

[13] Han X F, Jin H M, Wang Z J, Zhao T S and Sun C C 1993 *Phys. Rev.* B **47** 3248

[14] Zhang L G, Shen B G, Zhang S Y and Zhang H W 1998 *Acta Phys. Sin.* **47** 233 (in Chinese)

[15] Clausen K and Lebech B 1982 *J.Phys.* C: *Solid State Phys.* **15** 5095.

[16] Yamada M, Kato H, Yamamoto H and Nakagawa Y 1988 *Phys. Rev.* B **38** 620

[17] Liebs M, Hummler K and Fahnle M 1993 *J. Magn. Magn. Mater.* **124** 239.

[18] Fahnle M, Hummler K, Liebs M and Beuerle T 1993 *Appl. Phys.* A **57** 67

[19] Belorizky E, Fremy M A, Gavigan J P, Givord D and Li H S 1987 *J. Appl. Phys.* **61** 3971

[20] Loewenhaupt M and Sosnowska I 1991 *J. Appl. Phys.* **70** 5967